

Assessment of Internal Oxidation (IO) as a Mechanism for Submodes of Stress Corrosion Cracking that Occur on the Secondary Side of Steam Generators

Argonne National Laboratory

**U.S. Nuclear Regulatory Commission
Office of Nuclear Regulatory Research
Washington, DC 20555-0001**



Assessment of Internal Oxidation (IO) as a Mechanism for Submodes of Stress Corrosion Cracking (SCC) that Occur on the Secondary Side of Steam Generators

Manuscript Completed: April 2005

Date Published: October 2006

Prepared by

Dr. Roger W. Staehle, Consultant
22 Red Fox Road
North Oaks, MN 55127
USA

Under Contract to
Argonne National Laboratory
9700 South Cass Avenue
Argonne, IL 60439

Todd Mintz, NRC Project Manager

Prepared for
Division of Fuel, Engineering & Radiological Research
Office of Nuclear Regulatory Research
U.S. Nuclear Regulatory Commission
Washington, DC 20555-0001
NRC Job Code Y6588



**ASSESSMENT OF INTERNAL OXIDATION (IO) AS A MECHANISM FOR
SUBMODES OF SCC THAT OCCUR ON THE SECONDARY SIDE OF STEAM
GENERATORS**

by

Roger W. Staehle
Adjunct Professor
University of Minnesota

ABSTRACT

A mechanism of “internal oxidation” (IO) is assessed for its applicability to interpreting the stress corrosion cracking (SCC) of high nickel alloys in high temperature deaerated water. This submode of SCC is “low potential stress corrosion cracking” (LPSCC). The applicability of the IO mechanism to LPSCC is assessed mainly with respect to the dependence of LPSCC on electrochemical potential and on the diffusivity of oxygen in grain boundaries. For these two considerations, IO does not provide quantitative interpretations of LPSCC.

FOREWORD

The work discussed in this report was conducted for the U.S. Nuclear Regulatory Commission (NRC), Office of Nuclear Regulatory Research, Division of Engineering Technology, Materials Engineering Branch, by Dr. Roger W. Staehle of Staehle Consulting, under a subcontract from Argonne National Laboratory.

This report assesses the relevance of the internal oxidation (IO) model in predicting the occurrence of primary water stress corrosion cracking (PWSCC) (also referred to as low-potential stress corrosion cracking) in steam generator tube materials fabricated from Alloy 600 and similar alloys. Having an accurate set of models for stress corrosion cracking (SCC) provides a basis for the NRC to establish inspection intervals for eddy current testing of steam generator tubes, and aids in conducting operational assessments of steam generators. SCC occurs in three stages, which include initiation, evolution, and growth. All three stages are important to understand for determining inspection intervals and conducting operational assessments. The various growth models can be used to determine the probability of exceeding the acceptance criteria for stress corrosion cracks during the next operating cycle.

The IO model is based on the assumption that oxygen produced by the reduction of water diffuses into the grain boundaries of the steam generator tube material and results in local embrittlement of the grain boundaries. The fracture of those boundaries, in turn, results in the formation of intergranular SCC. Dr. Staehle proposes that PWSCC is not dependent on the presence of oxygen. He further proposes that the rate of diffusion of oxygen into the grain boundaries is not rapid enough to account for the crack growth rate associated with PWSCC. For these reasons, Dr. Staehle does not believe that the IO model is applicable to explain PWSCC. Many researchers still believe that the IO model does provide an explanation for PWSCC. The NRC recognizes the complex nature of SCC and has not taken a position on this issue. However, the information from this and other reports will be of use in further research to better understand SCC.

The insights from this literature review will be considered as Argonne National Laboratory develops SCC models for the NRC. In particular, the model being developed for PWSCC (and other models for SCC) is expected to yield information for use in predicting the probable first occurrence of SCC for a given material/chemistry combination. In addition to providing such information on initiation, other models are expected to yield information on the evolution and growth of cracks that do initiate. Given the large variation in initiation times and crack growth rates, statistical models that are physically based will be developed in an attempt to provide realistic estimates of initiation times and crack growth rates.



Carl J. Paperiello, Director
Office of Nuclear Regulatory Research
U.S. Nuclear Regulatory Commission

TABLE OF CONTENTS

	PAGE
ABSTRACT	iii
FOREWORD.....	v
LIST OF FIGURES	viii
EXECUTIVE SUMMARY	xi
ACKNOWLEDGEMENTS	xii
ACRONYMS AND ABBREVIATIONS	xiii
1.0 INTRODUCTION.....	1
2.0 SUPPORT FOR THE IO MODEL.....	4
3.0 OBJECTIONS TO THE IO MODEL.....	7
3.1 Dependence upon Potential.....	7
3.2 Rate of Diffusion.....	13
3.3 Other Objections	14
4.0 ASSESSMENT	16
5.0 CONCLUSIONS.....	18
6.0 REFERENCES.....	19

LIST OF FIGURES

	PAGE
1. Major submodes of SCC and IGC for Alloy 600 in sensitized and mill annealed conditions in the range of 280° to 350°C in aqueous solutions. Regions of SCC shown with respect to thermodynamic boundaries for iron and nickel species in water. LPSCC = “low potential SCC.” HPSCC = “high potential SCC.” AkSCC = “alkaline SCC.” AcSCC = “acidic SCC.” SN = “sensitized.” MA = “mill annealed.” P = “pure water.” C = “contaminated.”.....	2
2. Periodic rupture at grain boundaries associated with diffusion of oxygen as applied to a Ni-Al alloy.	3
3. Crack growth rate vs. 1/T for various nickel base alloys including the oxygen induced cracking of Ni ₃ Al and the IGSCC of Alloys 600, X-750, and 718.	5
4. Plateau crack growth rate vs. 1/T for Alloys 600 and 750 in water and steam together with Ni ₃ Al in oxygen.	6
5. (a) Schematic view of an advancing SCC relative to possible ranges of potential, being aerated or deaerated, defined by the Ni-H ₂ O potential-pH diagram. (b) Potential-pH diagram for Ni-H ₂ O at 300°C. (c) Schematic view of a heat transfer crevice relative to possible ranges of potential defined by the potential-pH diagram for Ni-H ₂ O.....	8
6. (a) Percent of fracture surface with IGSCC as a function of applied potential for Alloy 600 tested at 350°C using SSRT for two pressures of hydrogen. (b) Time to 30% IGSCC vs. hydrogen pressure and potential reference to NiO/Ni equilibrium. Experiments at 400°C and 205 atm pressure of steam. (c) Crack growth rate at two stress intensities vs. potential (E_cP =electrochemical potential) relative to the NiO/Ni equilibrium potential for Alloy 600MA at 338°C. (d) Crack growth rate vs. hydrogen pressure for Alloy 600 at 330°C using CERT at $6.67 \times 10^{-8} \text{ s}^{-1}$. (e) Crack growth rate vs. hydrogen concentration for Alloy 600MA at two temperatures in simulated primary water obtained using SSRT. (f) Crack growth rate vs. hydrogen concentration for Alloy 600MA at 288°C and with a stress intensity of 25 Ksi in ^{-1/2} . Some of the plots have been reversed from their original publication in order to permit self consistent comparisons; low potentials (high hydrogen) are shown at the left for all figures (a) through (f).....	9 & 10
7. Crack propagation rate vs. potential for Type 304 stainless steel and Alloy 600 both in the sensitized conditions at higher potentials and Alloy 600MA at two stress intensities at lower potentials. Data for Alloy 600MA are normalized to BWR conditions using $Q=40 \text{ kcal/mol}$ and applying at BWR pH. Data for sensitized materials taken from Ford and Andresen; ⁴⁹ data for Alloy 600MA taken from Figure 6c.	11

8.	(a) Electrochemical potential vs. log of oxygen solubility in nickel determined at pH 8 and 600°K. Compounds based on alloying elements in Alloy 600 that react to form oxides. (b) Crack growth rate at two stress intensities vs. potential (E_cP =electrochemical potential) relative to the NiO/Ni equilibrium potential for Alloy 600MA at 338°C.	12
9.	Depth of grain boundary penetration after time of exposure in Ni-270 vs. $1/T$ (absolute temperature). Correlation lines based on least squares.	13
10.	Diffusion coefficient vs. $1/T$ for oxygen in nickel from various researchers.	14
11.	Depth of oxygen penetration vs. time for selected temperatures from combined data of various researchers.....	17

EXECUTIVE SUMMARY

The purpose of this report is to assess the relevance of the internal oxidation (IO) model to predicting the occurrence of low potential SCC or to any of the submodes of SCC as it relates to Alloy 600 and similar alloys. IO has been proposed as a model for interpreting the submode of low potential SCC (LPSCC) as it occurs on the primary side of tubing in PWRs. This model may also apply to the secondary side of SGs as LPSCC may occur in less pure water characteristic of heat transfer deposits.

The proposed mechanism of IO applied to LPSCC is based on the concept that oxygen from the reduction of water can diffuse into the grain boundaries and produce local embrittlement. Support for this interpretation comes from the similarity of activation energies of LPSCC and similar processes known to sustain IO at higher temperatures. Also, there is some qualitative similarity to lower temperature data from diffusion of oxygen in the grain boundaries of pure nickel. Finally, experiments have shown that low oxygen activities in the range of the NiO/Ni equilibrium half cell can produce intergranular penetrations that could relate to the early stage of LPSCC related to IO.

Quantitative analysis of the IO mechanism in this report shows that it is not applicable to interpreting LPSCC or any of the submodes of SCC that have been presently observed. The principal objections are the following:

1. The dependence of LPSCC on potential does not follow the solubility of oxygen as a function of potential.
2. The diffusivity of oxygen is not sufficiently rapid to account for the velocity of LPSCC as well as other more rapidly propagating submodes.

ACKNOWLEDGEMENTS

In preparing this NUREG I am indebted to discussions with Steve Bruemmer of PNL, Rick Eaker of Duke Power, Zhi Fang of Medtronic Corporation, Bob Hermer of Bechtel Bettis Inc., Tracy Gendron of AECL, Jeff Gorman of Dominion Engineering, Mac Hall of Bechtel Bettis Inc., Nathan Lewis of KAPL Inc., Al McIlree of EPRI, Howard Pickering of the Pennsylvania State University, Bob Rapp of The Ohio State University, Dewey Rochester of Duke Power, Larry Thomas of PNL, Charles Thompson of KAPL Inc., and Gary Was of the University of Michigan.

I am particularly indebted to Peter Scott of Framatome for many productive discussions on this and other related subjects.

Finally, I am indebted to the professionalism of my office staff in assisting with the preparation of this report: Mary Elizabeth Ilg, Barbara Lea, Julie Daugherty, Tim Springfield, and Erin Kate Rediger. The graphics for this paper were prepared by John Ilg.

ACRONYMS AND ABBREVIATIONS

AcSCC	Acidic Stress Corrosion Cracking
AlkSCC	Alkaline Stress Corrosion Cracking
BWR	Boiling Water Reactor
C	Contaminated
CERT	Constant Extension Rate Test
HPSCC	High Potential Stress Corrosion Cracking
IGSCC	Intergranular Stress Corrosion Cracking
IO	Internal Oxidation
LPSCC	Low Potential Stress Corrosion Cracking
OTSG	Once-Through Steam Generator
MA	Mill Annealed
P	Pure Water
SCC	Stress Corrosion Cracking
SN	Sensitized
SSRT	Slow Strain Rate Test

1.0 INTRODUCTION

The purpose of this discussion is to assess and review the mechanism of internal oxidation (IO) as an explanation for the LPSCC of Alloy 600 together with questions that have been raised about the applicability of this model. While LPSCC has been nominally a problem for the primary side of PWR steam generators, it may be important also for interpreting SCC on the secondary side. The concept of IO as applied to explaining the mechanism of LPSCC was proposed by Scott and Le Calvar¹ and further discussed by Gourgues et al.² The application of IO to interpreting LPSCC on the secondary side of steam generators is described by Rochester and Eaker.³ Questions concerning the applicability of IO to interpreting LPSCC were raised by Staehle and Fang.⁴

LPSCC occurs in the range of potentials close to the NiO/Ni equilibrium half cell. This upper boundary has been reproducibly defined first by Smialowska et al.⁵ and Totsuka and Smialowska.⁶ The range of pH over which LPSCC occurs has not been extensively investigated except for various studies in pure and primary water. Smialowska et al.⁵ have shown that LPSCC occurs over the pH range of 3.4 to 9.0. Figure 1 shows the general range of occurrence of LPSCC relative to other submodes including AkSCC, AcSCC, and HPSCC. LPSCC is clearly different from the other submodes of SCC with respect to the ranges of potential and pH over which it occurs. Whatever mechanistic interpretation applies to LPSCC must account for these differences.

Scott and Le Calvar¹ examined the several prominent mechanisms for explaining LPSCC. They concluded that mechanisms related to anodic dissolution, hydrogen, and bubble formation could not explain the observed kinetics of LPSCC. On the other hand, they suggested evidence that the IO process was the most likely to be consistent with the observed dependencies of LPSCC.

Since the time of this proposal by Scott and Le Calvar for IO explaining LPSCC, Scott has refined his view of key processes at the tip of LPSCC and considers that the formation of porosity is critical to developing a useful mechanism.^a This porosity has been identified using the ATEM by Bruemmer and Thomas.⁷ Nonetheless, the idea of diffusion of oxygen in the grain boundary is an important mechanistic consideration, and this idea is assessed in this report.

Scott and Le Calvar propose that oxygen diffuses along grain boundaries and produces an embrittling effect as proposed by Hipsley and DeVan.⁸ Such an effect might result from the formation of brittle phases or from the direct weakening by the presence of oxygen. A schematic view of such a process is shown from Hipsley and DeVan⁸ in Figure 2. This embrittling process at grain boundaries, involving the formation of a brittle zone followed by its fracture, is generally similar to that proposed by Forty and Humble⁹ for explaining the SCC of copper base alloys although the mechanism for forming the brittle layer is different. The brittle film rupture mechanism has been elaborated upon extensively by Pugh as it applies to copper alloys.¹⁰

^aP. Scott, personal communication, April 24, 2002.

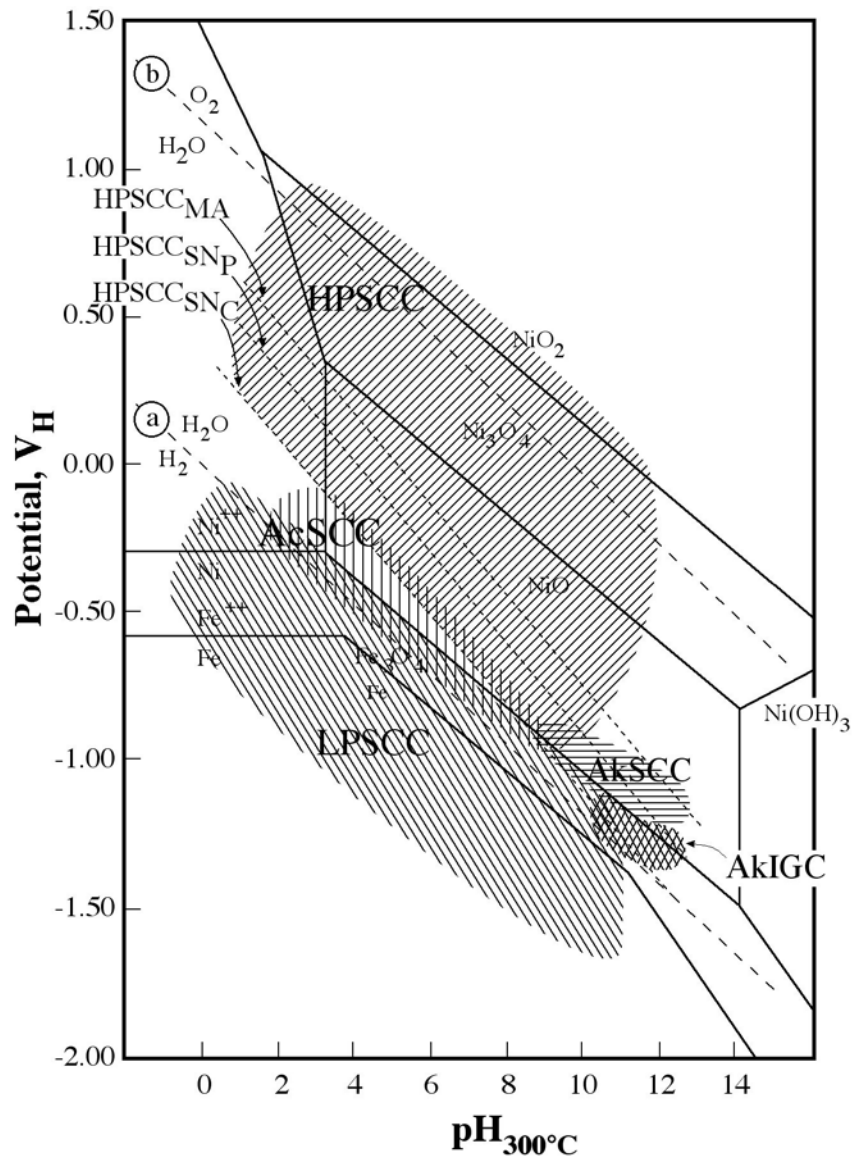


Figure 1 Major submodes of SCC and IGC for Alloy 600 in sensitized and mill annealed conditions in the range of 280° to 350°C in aqueous solutions. Estimated regions of SCC shown with respect to thermodynamic boundaries for iron and nickel species in water. LPSCC = “low potential SCC.” HPSCC = “high potential SCC.” AKSCC = “alkaline SCC.” AcSCC = “acidic SCC.” SN = “sensitized.” MA = “mill annealed.” P = “pure water.” C = “contaminated.”

Scott and Le Calvar¹ suggest that the IO model is relevant to LPSCC for two reasons:

1. LPSCC occurs generally close to the NiO/Ni half cell equilibrium where they suggest that oxygen can enter easily owing to the instability of the NiO.
2. The P_{O_2} is low as required to avoid forming a barrier layer of Cr_2O_3 .

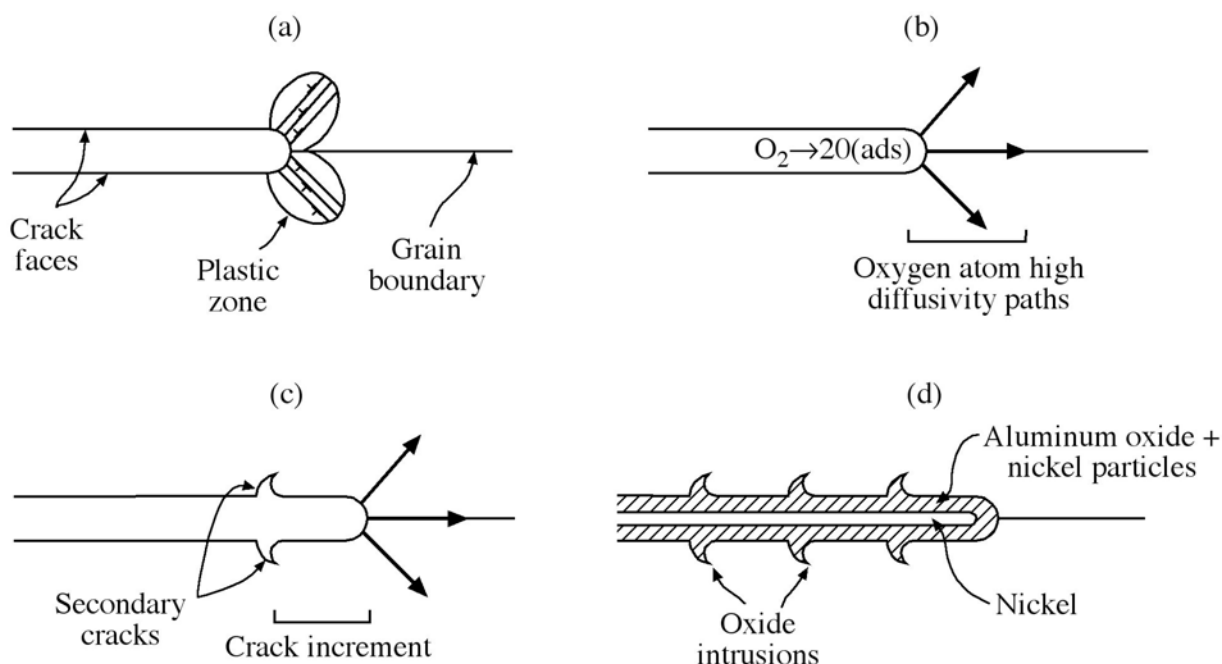


Figure 2 Periodic rupture at grain boundaries associated with diffusion of oxygen as applied to a Ni-Al alloy. From Hippsley and De Van.⁸ © 1989 Elsevier Science.

It is not clear that the IO model is an internal oxidation process as described by Meijering and Druyvesteyn,¹¹ Wagner,^{12,13} Rapp,^{14,15} and Swisher.¹⁶ Scott agrees that the IO mechanism as described by Scott and Le Calvar may not be a strictly internal oxidation process.^a In internal oxidation, as it is understood in oxidation studies, a more active alloy constituent reacts with the incoming oxygen to produce a reaction front consisting of the resulting oxide. The IO model proposed by Scott, however, involves more of an embrittlement due to the relatively high local oxygen at grain boundaries. Whether oxygen actually reacts with chromium ahead of the crack is not clear since the high nickel alloys sustain LPSCC in Ni-Cr-Fe alloys with Cr as low as 1 and 2%.¹⁷ However, the model being discussed here is referred to as an IO process, as it includes embrittlement at grain boundaries due to diffusion of oxygen, as compared with other mechanisms, such as those involving hydrogen, that have been proposed to explain LPSCC.

This discussion first identifies possible support for the IO mechanism; next the objections are identified.

^aP. Scott, personal communication, April 24, 2002.

2.0 SUPPORT FOR THE IO MODEL

After the publication of the Scott and Le Calvar and Gourgues et al. papers, the IO model was proposed by Rochester and Eaker³ as an interpretation of SCC on the secondary side of OTSGs where it had been observed extensively on the free span. The occurrence of LPSCC on the secondary side could be rationalized by the presence of hydrazine that could lower the electrochemical potential into the LPSCC range. The IO model thus received additional interest and scrutiny in connection with that application. The support for the IO model here is taken both from the early papers of Scott and co-workers as well as from the work in connection with the interpretation of the SCC in OTSGs.

The essential support for the IO model advanced by Scott and Le Calvar¹ includes the following:

1. Oxygen might diffuse in nickel grain boundaries at rates that approach those of LPSCC based on data in the papers of Woodford and co-workers.^{18,19} Figure 3 shows data from Scott^b that indicate a good correlation between the data in oxygen, where a grain boundary oxygen embrittlement was observed, and the IGSCC of high nickel alloys in water. The role of oxygen diffusing in grain boundaries to promote embrittlement has been described by Hipsley and De Van as shown in Figure 2.⁸
2. The only direct data for the diffusion of oxygen in nickel base alloys is from Bricknell and Woodford¹⁸ and Iacocca and Woodford.¹⁹ These data, if taken together, (as discussed in Section 3.2 in connection with Figure 9), exhibit a slope that is similar to that of Barlow and Grundy²⁰ for the diffusion of oxygen in polycrystals and single crystals as shown in Figure 3 and also in Figure 10. Scott suggests that the most relevant of the Bricknell and Woodford and Iacocca and Woodford work might be the lower temperature points. With these, Scott proposes a line, given as #4, that corresponds well with the Hipsley and De Van⁸ data in Figure 3 and correlates well with the LPSCC of Alloy 600. While the rates shown by taking all of the data from Woodford and co-workers are not adequate to rationalize IO as shown in Figure 3, Scott^b has suggested that the additional diffusivity necessary might be rationalized by effects of stress on diffusivity. This work is described in six studies.^{21,22,23,24,25,26}
3. Scott has also shown that the temperature dependence of the Ni₃Al work of Hipsley and De Van is similar to that of other work on Alloys 600 and 750 for crack growth as shown in Figure 4.^b
4. Scott and Le Calvar¹ note that there might be some under-prediction, as suggested in Figure 3, based on the Woodford data, due to trapping of oxygen in the pure nickel that may change the specific applicability to LPSCC.

^bP. Scott, presentation at EPRI-Duke meeting to discuss IGC-SCC at Oconee on June 28, 1998.

5. Work by Wood and co-workers^{27,28,29,30} on the conventional internal oxidation in Ni-Cr alloys shows phenomena that are qualitatively similar to the proposed IO model.
6. The work of Gourgues et al.² showed that grain boundary cracking in the range of 10 μ m could be produced at 360°C on Alloy 600 in primary water. Similar results were shown by Gendron^{31,32,33,34,35} for 400°C although her work did not reproduce that of Gourgues at lower temperatures. Similar work was also conducted by Cassagne et al.³⁶
7. Studies of photomicrographs from the Oconee OTSG SCC indicated tight cracks that seemed too tight to be rationalized by access to the environment and seemed to support the diffusion of oxygen inward for significant distances.³ Further, initial work indicated that only oxygen, as might be related to internal oxidation, was present in these boundaries.

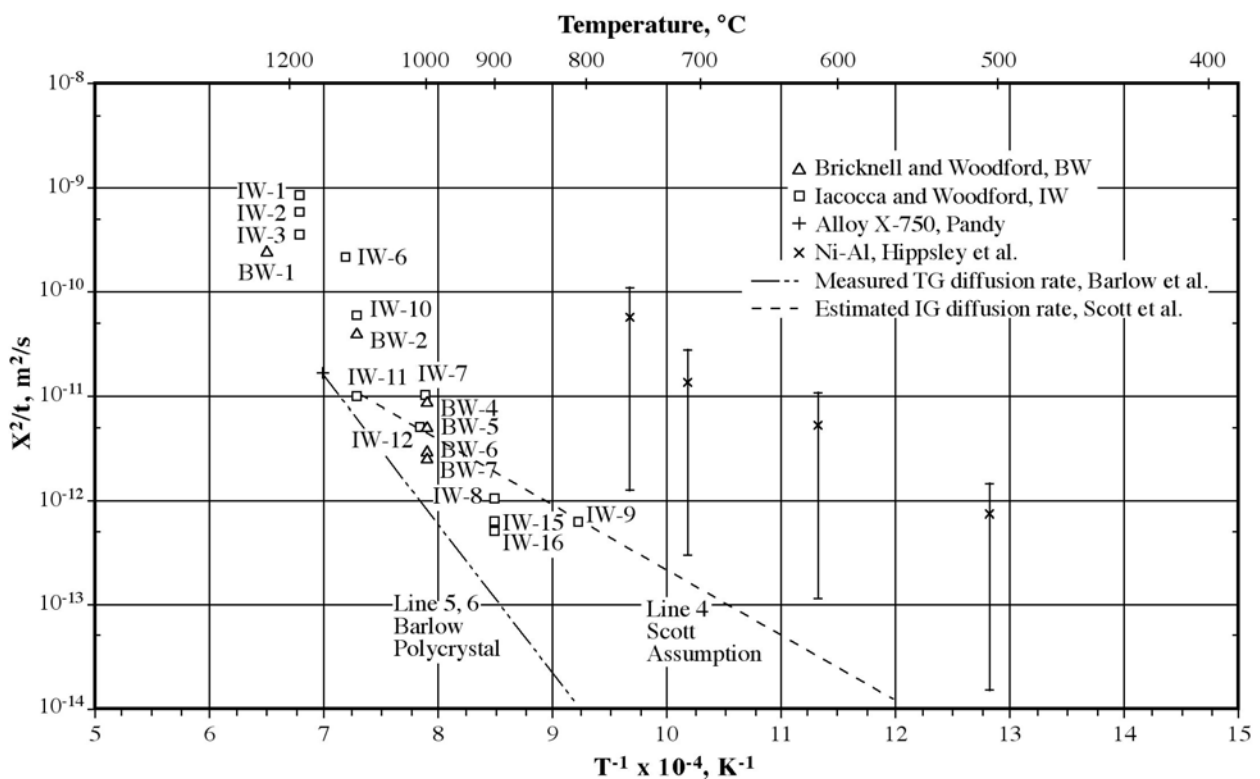


Figure 3 Crack growth rate vs. 1/T for various nickel base alloys including the oxygen induced cracking of Ni₃Al and the IGSCC of Alloys 600, X-750, and 718. From Scott.^b

8. ATEM work³ in connection with OTSG studies indicated the presence of reactions near the crack tip that would suggest reactions with oxygen in the solid state. These included the oxidation of carbides and the formation of porous sponge.

^bP. Scott, presentation at EPRI-Duke meeting to discuss IGC-SCC at Oconee on June 28, 1998.

9. LPSCC seems to exhibit a preference for occurrence around the NiO/Ni line based on the early work of Economy et al.³⁷ This pattern suggests that this location is related to an adequate pressure of oxygen and a simultaneous weakness in the protective film that permits entry of oxygen.
10. The observations that Alloy 690 does not sustain LPSCC suggest that chromium acts to slow the diffusion of oxygen along grain boundaries.

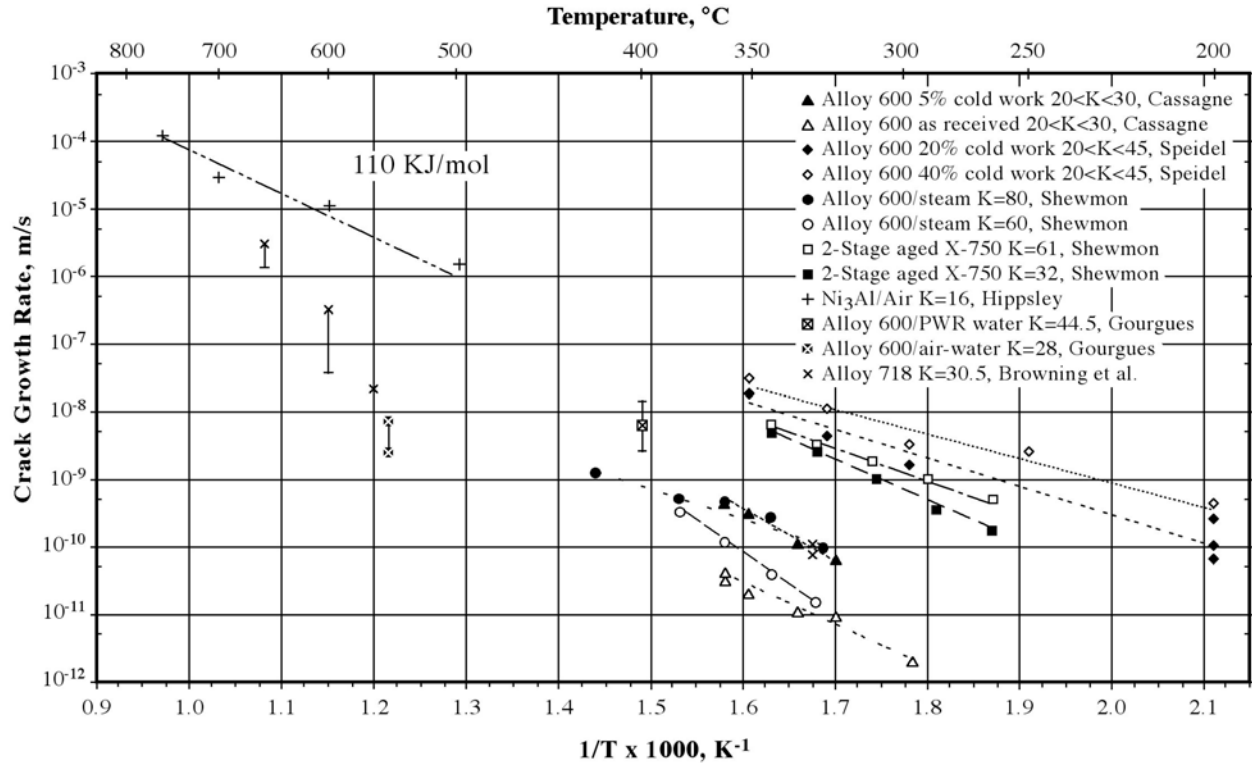


Figure 4 Plateau crack growth rate vs. $1/T$ for Alloys 600 and 750 in water and steam together with Ni_3Al in oxygen. From Scott.^b

^bP. Scott, presentation at EPRI-Duke meeting to discuss IGC-SCC at Oconee on June 28, 1998.

3.0 OBJECTIONS TO THE IO MODEL

The principal objections to the IO model and the background for these objections have been described by Staehle and Fang.⁴ They noted that there are two essential objections: one related to the dependence of LPSCC on potential as compared with oxygen pressure that is discussed in Section 3.1 and the other related to the diffusivity of oxygen that is discussed in Section 3.2. Other objections that address some of the nominally supportive elements of Section 2.0 are discussed in Section 3.3.

3.1 Dependence upon Potential

This section gives some background on the dependence of LPSCC on potential and discusses specifically an objection to the IO model in terms of its dependence upon potential.

The occurrence of LPSCC related to the variables of potential and pH as well as the occurrence of AkSCC, AcSCC and HPSCC are shown in Figure 1 for Alloy 600MA in the range of 300°C. This diagram shows why LPSCC is given this term of “low potential SCC” to contrast it with “high potential SCC.” The difference between these two submodes has been studied by Smialowska et al.,⁵ Shoji³⁸ and others. LPSCC is mostly related to the primary side of PWR steam generators and HPSCC is mostly related to BWRs in normal water chemistry. The AkSCC and AcSCC are generally related to heat transfer crevices in PWR steam generators. Other submodes including PbSCC are described by Staehle and Gorman.³⁹ However, there is no reason that LPSCC cannot occur on the secondary side although possibly modified by more complex chemistries than the relatively pure environments usually associated with this submode.

Part of defining LPSCC is related to the range of potential in which it functions as well as the dependence of LPSCC on potential. The range of potential in which LPSCC operates in primary as well as secondary systems is defined by the deaerated condition. Figure 5 shows the limitations of potential in deaerated primary and secondary systems for SCC as well as heat transfer crevices. Here, the highest potential that is achievable in a deaerated system is defined by the H_2O/H_2 half cell equilibrium as affected by the hydrogen pressure. The lowest potential is defined by the NiO/Ni half cell equilibrium which depends on pH and is invariant with potential. This lower potential can be slightly altered by the presence of iron and chromium; however, these contributions have appeared to be small. Nonetheless, mixed oxides are observed on the surface of Alloy 600 and appear to be more dominant than NiO . The lower potential can also be affected by the presence of hydrazine owing to its low half cell equilibrium potential. This contribution seems mainly to lower the possibly higher potentials that result from the low hydrogen on the secondary side.

Figure 5 indicates that there is little difference between the potentials at the surface and inside the advancing LPSCC. This is different from conditions where oxygen is present due to radiolysis. Here, the potential is high on the outside but is at the mixed potential of deaerated solutions at the tip of the advancing crack. This gradient causes negative ions to diffuse inward.

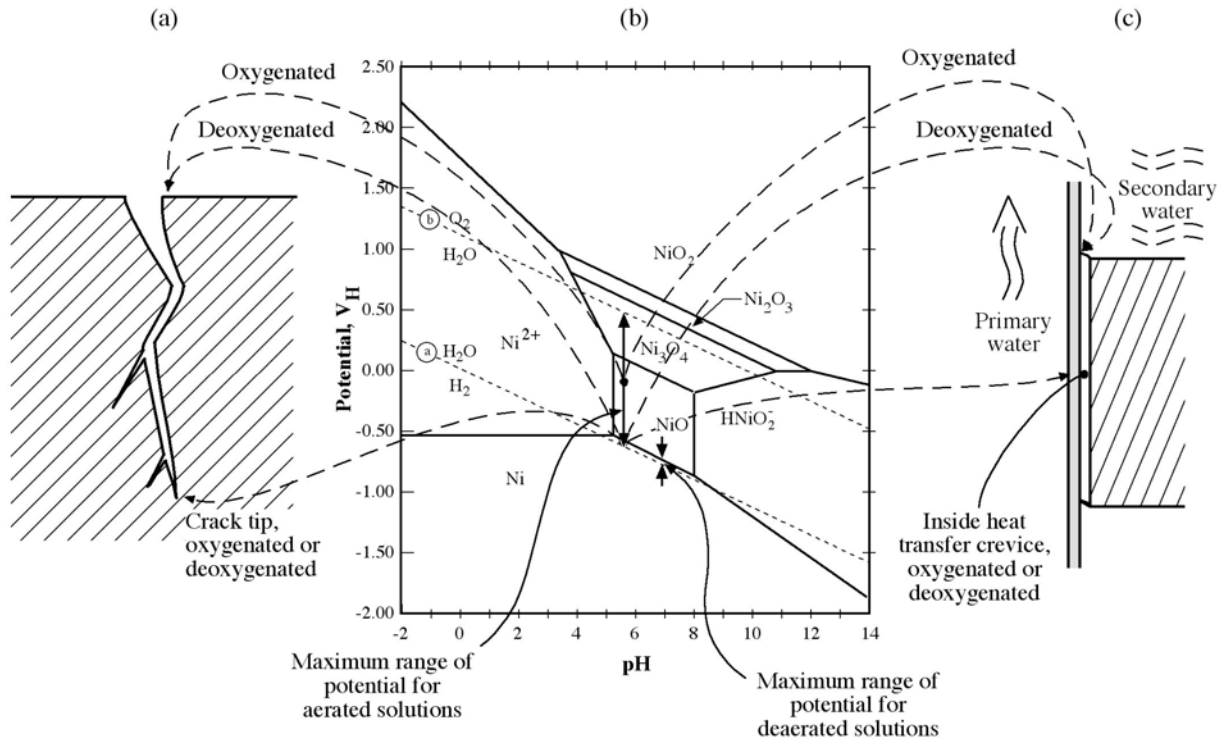


Figure 5 (a) Schematic view of an advancing SCC relative to possible ranges of potential, being aerated or deaerated, defined by the Ni-H₂O potential-pH diagram. (b) Potential-pH diagram for Ni-H₂O at 300°C. From Chen et al.⁴⁰ (c) Schematic view of a heat transfer crevice relative to possible ranges of potential defined by the potential-pH diagram for Ni-H₂O.

LPSCC has been studied as a function of potential, and results are shown in Figure 6.^{37,41,42,43,44,45,46} This dependence was first studied by Totsuka and Smialowska⁴¹ using applied potentials, and their results are shown in Figure 6a. Essentially, they show that LPSCC starts above the NiO/Ni half cell equilibrium and increases rapidly over about 100 mV and then becomes constant with decreasing potential. The next work by Economy et al.³⁷ in Figure 6b using hydrogen pressure to control the potential showed that LPSCC exhibits an approximately parabolic pattern with the NiO/Ni half cell equilibrium at the most rapid rate. Subsequently, other work has confirmed the work of Economy et al and has shown that the most rapid rate of LPSCC occurs at about the NiO/Ni equilibrium potential as shown in Figures 6 c-f.

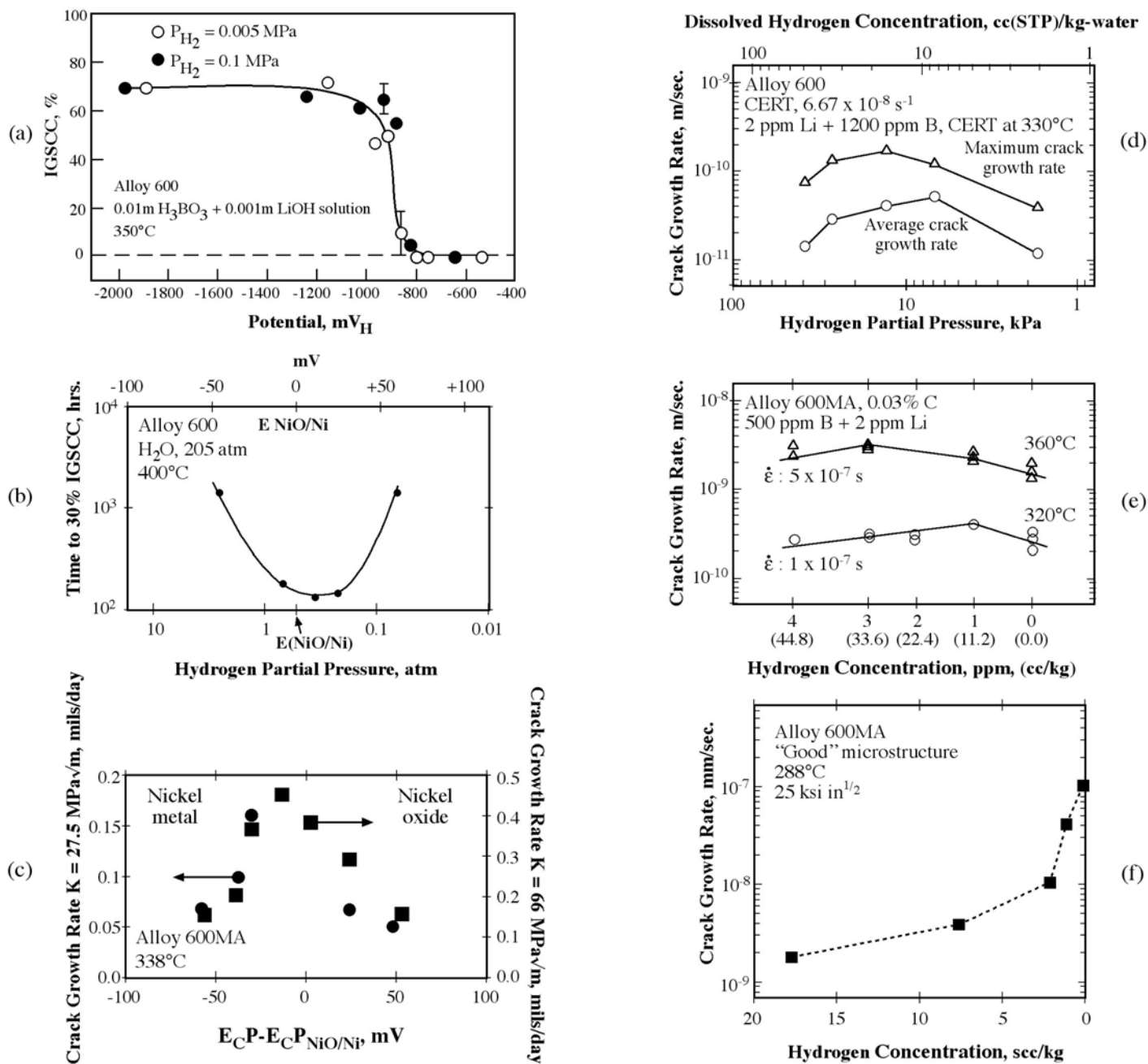


Fig. 6. Caption on next page.

Figure 6 (a) Percent of fracture surface with IGSCC as a function of applied potential for Alloy 600 tested at 350°C using SSRT for two pressures of hydrogen. From Totsuka and Smialowska.⁴¹ Courtesy of TMS, Warrendale, PA, USA. (b) Time to 30% IGSCC vs. hydrogen pressure and potential reference to NiO/Ni equilibrium. Experiments at 400°C and 205 atm pressure of steam. Original data from Economy et al.³⁷ Data recalculated by Scott and Combrade.⁴² © 1997 by the American Nuclear Society, La Grange Park, Illinois. (c) Crack growth rate at two stress intensities vs. potential (E_{CP} =electrochemical potential) relative to the NiO/Ni equilibrium potential for Alloy 600MA at 338°C. From Morton et al.⁴³ © 2002 NACE International. (d) Crack growth rate vs. hydrogen pressure for Alloy 600 at 330°C using CERT at $6.67 \times 10^{-8} \text{ s}^{-1}$. From Lee et al.⁴⁴ © 2002 NACE International. (e) Crack growth rate vs. hydrogen concentration for Alloy 600MA at two temperatures in simulated primary water obtained using SSRT. From Totsuka et al.⁴⁵ © 2002 NACE International. (f) Crack growth rate vs. hydrogen concentration for Alloy 600MA at 288°C and with a stress intensity of 25 Ksi in^{1/2}. From Andresen and Angeliu.⁴⁶ © 1997 NACE International. Some of the plots have been reversed from their original publication in order to permit self consistent comparisons; low potentials (high hydrogen) are shown at the left for all figures (a) through (f).

Andresen⁴⁷ has suggested that LPSCC and HPSCC are monotonically the same process from the point of view that Alloy 600 and Type 304 stainless steel in their sensitized conditions behave similarly. This hypothesis is explored in Figure 7 where Andresen's data are compared with data from Morton et al.⁴³ for crack growth rates. Here, the pH of the LPSCC data from Morton et al. are shifted along the NiO/Ni line and the temperature of these data was adjusted using an activation energy of 40 kcal/mol. This comparison shows that the patterns of SCC seem not to correspond. From this comparison it seems that there is no continuum between HPSCC and LPSCC. Thus, there appears to be no basis for considering that the same mechanism used to explain HPSCC applies to LPSCC.

The first objection to the IO model is based on the dependence of LPSCC upon potential. Figure 8b, which is taken from Figure 6c, shows one of a set of similar patterns in Figure 6. The essence of the first objection is shown in Figure 8a as compared with Figure 8b. Figure 8a provides a basis for assessing the dependence of dissolved oxygen at the metal surface as a function of potential. Figure 8a is evaluated at pH 8 and 600K. This plot is based on the solubility of oxygen in nickel as determined from an extrapolation of the work of Park and Alstetter⁴⁸ and applying Sieverts' Law. The pressure of oxygen is taken from the Nernst equation; combining these dependencies, as shown in Staehle and Fang,⁴ provides the dependence of the solubility on the potential. Figure 8b compares the dependence of LPSCC on potential with the effect of potential on the solubility of oxygen in Figure 8a.

To illustrate the application of Figure 8 to evaluating the IO mechanism, consider the NiO/Ni equilibrium shown at about -0.91 volts as a horizontal line. This line defines the potential below which Ni is stable and above which NiO is stable. A consequence of the region above this line is that the pressure of oxygen, and therefore the amount dissolved, is constant in equilibrium with NiO. Below this line the pressure of oxygen is not affected by the presence of NiO. The line

$E_o = E_o(p_{O_2})$ defines the Nernst pressure of oxygen. The intersection of this line with that for the NiO/Ni equilibrium half cell defines the solubility of oxygen in the metal in equilibrium with the potential in the absence of an oxide phase on the surface. There are three consequences of this intersection of the NiO/Ni and $E_o = E_o(p_{O_2})$ lines:

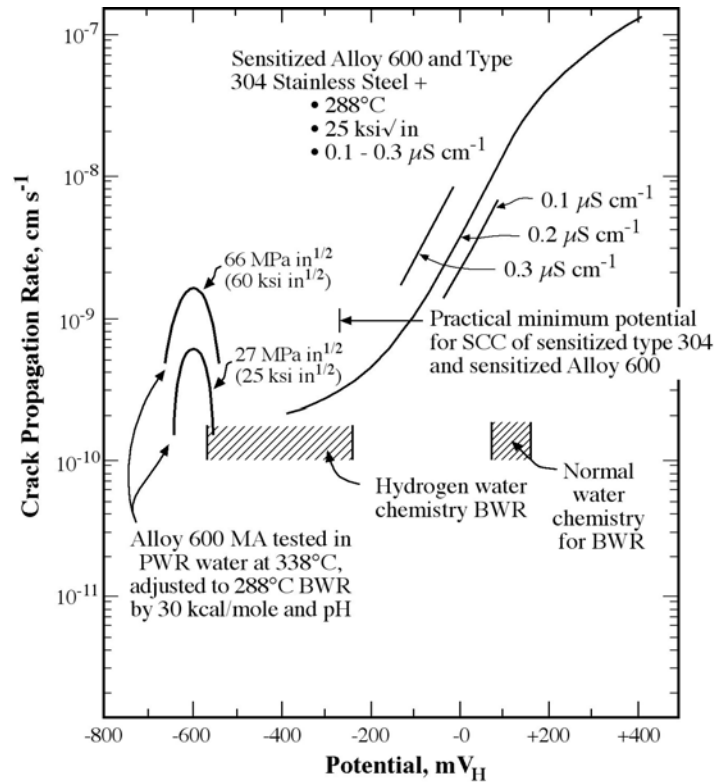


Figure 7 Crack propagation rate vs. potential for Type 304 stainless steel and Alloy 600 both in the sensitized conditions at higher potentials and Alloy 600MA at two stress intensities at lower potentials. Data for Alloy 600MA are normalized to BWR conditions using $Q=40$ kcal/mol and applying at BWR pH. Data for sensitized materials taken from Ford and Andresen;⁴⁹ data for Alloy 600MA taken from Figure 6c.

1. The solubility of oxygen in the metal is constant above the intersection.
2. The solubility of oxygen decreases rapidly below this intersection according to the line $E_o = E_o(p_{O_2})$.
3. If, instead of the dominant oxide being NiO, it is a mixed oxide, this transition occurs at a lower potential, and the solubility is much reduced above the potential at which the mixed oxide occurs.

Comparing the dependence of LPSCC in Figure 8b with the solubility of oxygen in Figure 8a shows the following:

1. The dependence of solubility of oxygen on potential exhibits no resemblance to the dependence of LPSCC on potential. If LPSCC were to depend on potential in the same way as the solubility of oxygen, LPSCC would extend to relatively high potentials and would be independent of potential above the intersection of the NiO/Ni and $E_o = E_o(p_{O_2})$ lines. Below this intersection LPSCC would follow the line $E_o = E_o(p_{O_2})$.

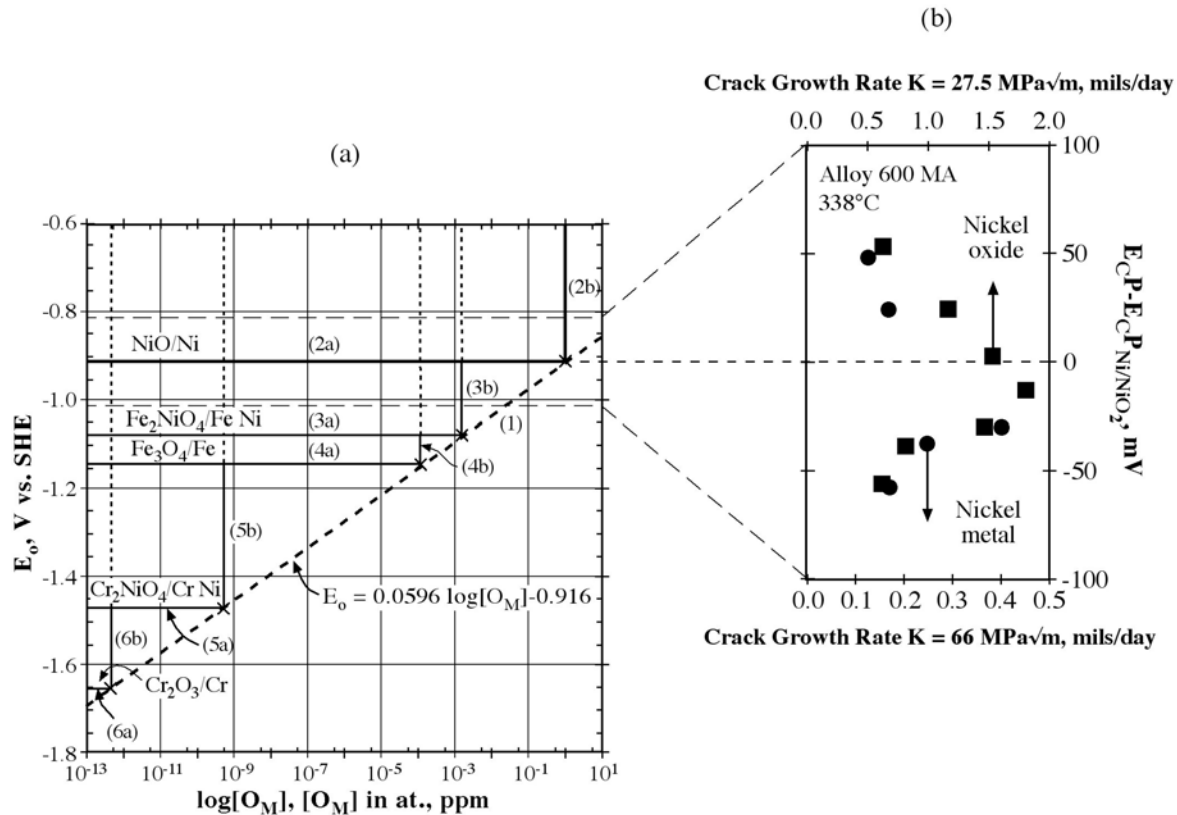


Figure 8 (a) Electrochemical potential vs. log of oxygen solubility in nickel determined at pH 8 and 600K. Compounds based on alloying elements in Alloy 600 that react to form oxides. From Staehle and Fang.⁴ Courtesy TMS, Warrendale, PA, USA. (b) Crack growth rate at two stress intensities vs. potential (E_{CP} =electrochemical potential) relative to the NiO/Ni equilibrium potential for Alloy 600MA at 338°C. From Morton et al.⁴³ © 2002 NACE International.

2. In view of the 15% Cr in Alloy 600, the oxide adjacent to the Alloy 600 surface is most likely a Ni-Cr mixed oxide. The equilibrium potential is shown as line 5a in Figure 8a. If the LPSCC were to be relevant to this oxide, the equilibrium solubility of oxygen above the intersection of lines would be very low, and the LPSCC would be independent of potential over the full range of potentials that are permitted in a deaerated system.

Thus, the lack of relationship between the dependence of potential for LPSCC and for oxygen solubility suggests that dissolved oxygen in the alloy is not relevant to LPSCC.

3.2 Rate of Diffusion

In connection with work in support of the OTSG problem as described by Rochester and Eaker,³ Scott prepared Figure 3^b that included some of the data of Woodford and co-workers. In developing a relationship between these data and LPSCC, he chose the lower temperature data. However, there does not appear to be a sound basis for this choice. The correlation of all of the data from Woodford and associates is shown in Figure 9, and this correlation is compared with that of Scott. Scott's correlation was based on values required to be consistent with the kinetics of LPSCC and was related to the lower temperature data of Woodford and co-workers. Whether Scott's approach is legitimate is not clear; however, it is not consistent with all of the data of Woodford and co-workers.

The question of consistency over a broad range of temperature for the diffusion of oxygen in nickel is addressed in Figure 10 where the available data for the diffusion of oxygen in polycrystalline nickel is given. Here, it appears that the diffusion of oxygen in nickel is linearly monotonic over a broad range of temperatures suggesting that all of the data of Woodford and his co-workers should be included in a correlation as shown in Figure 9.

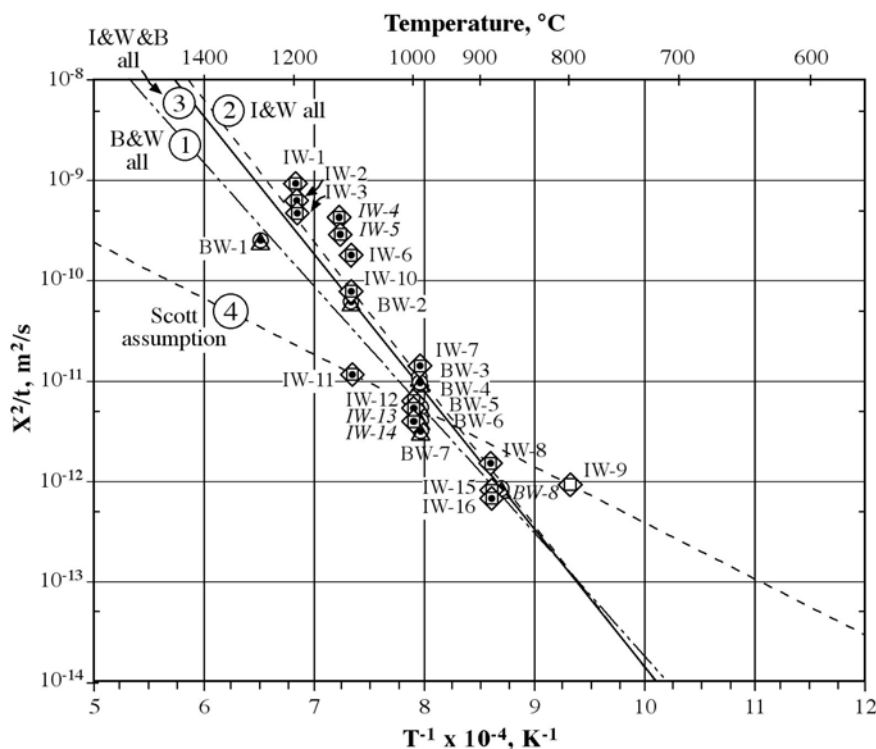


Figure 9 Depth of grain boundary penetration after time of exposure in Ni-270 vs. $1/T$ (absolute temperature). Data points from work of Bricknell and Woodford¹⁸ and Iacocca and Woodford.¹⁹ Correlation lines based on least squares. Line 4 from Scott.^b From Staehle and Fang.⁴ Courtesy TMS, Warrendale, PA, USA.

^bP. Scott, presentation at EPRI-Duke meeting to discuss IGC-SCC at Oconee on June 28, 1998.

If the full set of Woodford data are used, the penetration of oxygen with time can be calculated. The data based on Scott's line #4 (corresponds to the same in Figures 3, 9, and 10) are compared with data based on the complete Woodford et al. data in Figure 11. The data here at 300°C show that Scott's extrapolation based on Figure 3 predict more than three orders of magnitude greater penetration than predicted by using the full set of the Woodford data in Figure 9.

3.3 Other Objections

In addition to the major objections to the IO model from the points of view of dependence on potential and on diffusion of oxygen, there are other objections following some of the supporting points given in Section 2.0:

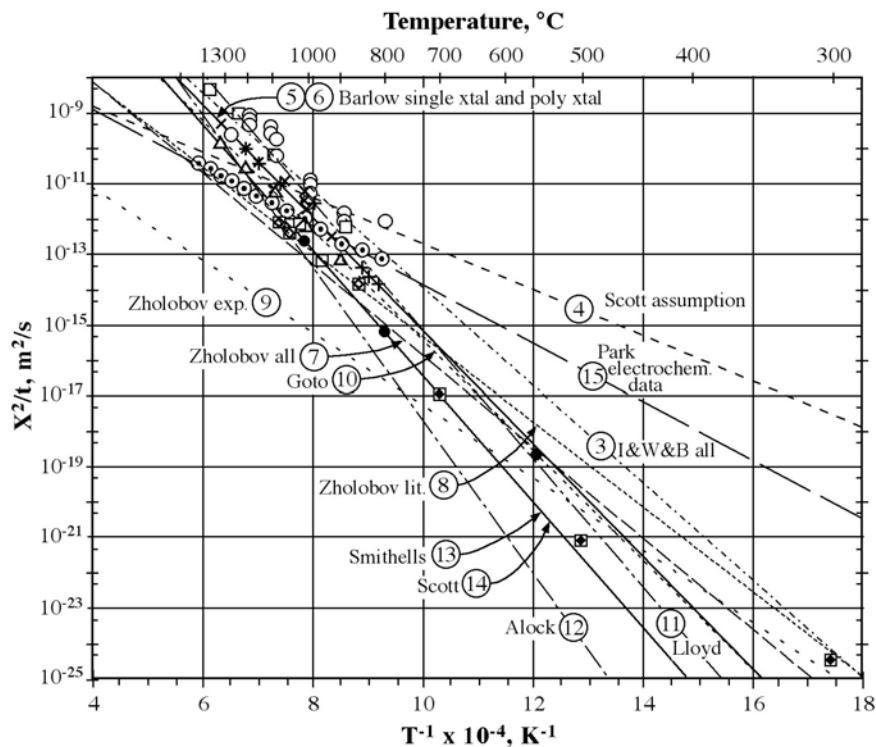


Figure 10 Diffusion coefficient vs. $1/T$ for oxygen in nickel from various researchers. Lines 3 and 4 are from Figure 9, from the work of Bricknell and Woodford,¹⁸ Iacocca and Woodford,¹⁹ and Scott.^b From Staehle and Fang.⁴ Courtesy TMS, Warrendale, PA, USA.

1. “Ghost Cracks”

While it seemed that the presence of very tight cracks provided evidence for long range diffusion of oxygen,³ these have been examined in detail and shown to be cracks that have direct access to the environment. They also exhibit the presence of species whose origin can only be the environment.⁵⁰

^b P. Scott, presentation at EPRI-Duke meeting to discuss IGC-SCC at Oconee on June 28, 1998.

2. Surface cracks

While Gourgues et al.,² Gendron,^{31,32,33,34,35} and Cassagne³⁶ demonstrated that short intergranular surface cracks can occur, these cracks did not propagate under the application of simultaneous stress.

3. Analytical Transmission Electron Microscopy (ATEM)

The ATEM work of Bruemmer and Thomas⁷ and Lewis et al.⁵¹ has not shown any evidence of oxidized species nor of oxygen ahead of crack tips.

4. Transgranular SCC (TGSCC)

Smialowska et al.⁵ demonstrated that some LPSCC can proceed in Alloy 600 by TGSCC at several different potentials and temperatures. Rebak et al.⁵² also found such TGSCC in cold worked material. These findings suggest that grain boundaries may not be the exclusive path of TGSCC.

5. LPSCC in low chromium Fe-Ni alloys

Yonezawa and Onimura¹⁷ show that LPSCC occurs in Ni-Cr-Fe alloys with 1 and 2% Cr. This suggests that Cr is not significant in the internal oxidation process although some IO systems require lower rather than higher concentrations of the active alloy species.

4.0 ASSESSMENT

The purpose of this discussion was to consider only the IO mechanism as proposed essentially by Scott and Le Calvar to explain LPSCC as shown in Figure 1. The purpose was not to review all mechanisms. In addition, the scope of this paper only considered LPSCC.

Any mechanism that is proposed for LPSCC must, at a minimum, explain the following phenomena:

1. The dependence upon potential as shown in Figures 1, 6, 7 and 8 including the nominally parabolic shape of the intensity of SCC shown in Figures 6b-f with the center being approximately at the NiO/Ni half cell equilibrium.
2. The apparently broad range of pH over which LPSCC occurs.
3. The difference from AkSCC, AcSCC, and HPSCC in both potential and pH dependence.
4. Dependencies on both Cr and Ni concentrations.
5. Stress and temperature dependencies.
6. The occurrence of TGSCC.
7. The occurrence, as well as the non-propagation, of the shallow intergranular penetrations observed in three different laboratories.^{2,31,32,33,34,35,36}

Since Scott now views the IO process as too slow to account for LPSCC,^b answering these questions may be moot. However, since the IO process is probably at least as interesting as other possible mechanisms for LPSCC and since there is no other mechanism available responding quantitatively to the seven questions raised in this section, a brief assessment is appropriate.

1. The IO mechanism does not fit the dependence of LPSCC on potential from the point of view of potential-dependent solubility of oxygen. This alone is probably sufficient to render the mechanism non-applicable.
2. The IO mechanism, as it depends on the diffusion of oxygen, does not fit the observed kinetics of LPSCC.
3. The low concentrations of Cr at which LPSCC occurs with relatively high intensities does not fit a model of IO.
4. No compounds or other structure is observed by ATEM ahead of the cracks.

^bP. Scott, presentation at EPRI-Duke meeting to discuss IGC-SCC at Oconee on June 28, 1998.

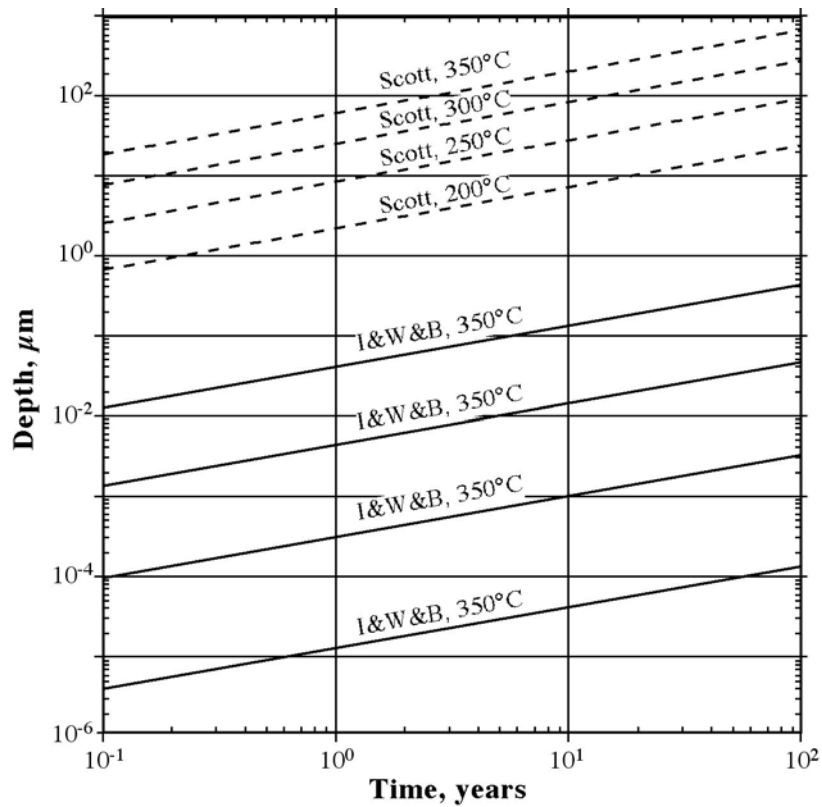


Figure 11 Depth of oxygen penetration vs. time for selected temperatures from combined data of Bricknell and Woodford;¹⁸ and Iacocca and Woodford;¹⁹ (line 3 in Figure 9) and from Scott^b (line 4 in Figure 9). From Staehle and Fang.⁴ Courtesy TMS, Warrendale, PA, USA.

5. The dependence of LPSCC on Cr seems to fit the expectation from an IO model in that increasing Cr would be expected to reduce the diffusivity of oxygen.
6. The non-propagating shallow intergranular cracks, especially over the range of potentials where they occur, are not explained by other than an IO type of mechanism although it is not clear that these are a part of the LPSCC process.
7. There is no good explanation for the parabolic shape of the intensity of LSPCC as a function of potential except by the qualitative arguments of Scott.

5.0 CONCLUSIONS

1. LPSCC cannot be implemented as an IO mechanism because:
 - the kinetics of diffusion of oxygen are substantially less than those for the propagation of LPSCC.
 - the dependence of LPSCC on potential differs substantially from the thermodynamically defined solubility of oxygen as a function of potential.
2. There are other mechanisms of crack advance that provide better models for LPSCC including hydrogen effects as formation of porous layers. However, arguments for the applicability of these options are not discussed here.

On balance, it appears that LPSCC cannot be interpreted by an IO mechanism. Also, it does not seem that mechanisms such as bubble formation, hydrogen entry, and film rupture supply more quantitative interpretations.

Scott's proposition that the formation of a porous layer at the crack tip may provide a better mechanistic interpretation and seems to be a more attractive avenue for study. Further, this process has been applied to other alloys in the same range of active/noble species with good success.⁵³ However, this mechanism is not part of the present discussion and is not elaborated upon.

6.0 REFERENCES

1. P. Scott and M. Le Calvar, "Some Possible Mechanisms of Intergranular Stress Corrosion Cracking of Alloy 600 in PWR Primary Water," Proceedings of the Sixth International Symposium on Environmental Degradation of Materials in Nuclear Power Systems - Water Reactors, R.E. Gold and E.P. Simonen, eds., The Mineral, Metals, and Materials Society (TMS), Warrendale, Pennsylvania, 1993, p. 657.
2. A. Gourgues, P. Scott, and E. Andrieu, "A Study of the Mechanism of Primary Water Stress Corrosion Cracking of Alloy 600," Seventh International Symposium on Environmental Degradation of Materials in Nuclear Power Systems - Water Reactors, G. Airey, et al., eds., NACE, Houston, Texas, 1995, p. 829.
3. D.P. Rochester and R.W. Eaker, "Laboratory Examination Results from Oconee Nuclear Station Once Through Steam Generation Tubes," Proceedings: Ninth International Symposium on Environmental Degradation of Materials in Nuclear Power Systems - Water Reactors, F.P. Ford, S.M. Bruemmer and G.S. Was, eds., The Mineral, Metals, and Materials Society (TMS), Warrendale, Pennsylvania, 1999, p. 639.
4. R.W. Staehle and Z. Fang, "Comments on a Proposed Mechanism of Internal Oxidation for Alloy 600 as Applied to Low Potential SCC," Proceedings of the Ninth International Symposium on Environmental Degradation of Materials in Nuclear Power Systems - Water Reactors, F.P. Ford, S.M. Bruemmer and G.S. Was, eds., The Mineral, Metals, and Materials Society (TMS), Warrendale, Pennsylvania, 1999, p. 69.
5. Z. Szklarska-Smialowska, Z. Xia, and R.R. Valbuena, "Mechanism of Crack Growth in Alloy 600 in High Temperature Deaerated Water," Corrosion 50, 1994, p. 76.
6. N. Totsuka and Z. Szklarska-Smialowska, "Effect of Electrode Potential on the Hydrogen-Induced IGSCC of Alloy 600 in an Aqueous Solution at 350°C," Corrosion 43, 1987, p. 734.
7. S.M. Bruemmer and L.E. Thomas, "Insights into Environmental Degradation Mechanisms from High-Resolution Characterization of Crack Tips," Proceedings: Chemistry and Electrochemistry of Stress Corrosion Cracking: A Symposium Honoring the Contributions of R.W. Staehle, R.H. Jones, ed., The Mineral, Metals, and Materials Society (TMS), Warrendale, Pennsylvania, 2001, p. 123.
8. C.A. Hipsley and J.H. De Van, "A Study of High Temperature Crack Growth in Nickel Aluminide," Acta Metallurgical 37, 1989, p. 1485.
9. A.J. Forty and P. Humble, "The Influence of Surface Tarnish on the Stress-Corrosion of α -Brass," Phil Mag. 8, 1963, p. 247.

10. E.N. Pugh, "The Stress Corrosion Cracking of Copper, Silver, and Gold Alloys," Fundamental Aspects of Stress Corrosion Cracking: NACE-1, R.W. Staehle, A.J. Forty and D. van Rooyen, eds., NACE, Houston, 1969, p. 118.
11. J.L. Meijering and M.J. Druyvesteyn, "Hardening of Metals by Internal Oxidation," Philips Research Reports 2, 1947, p. 81.
12. C. Wagner, "Internal Oxidation of Cu-Pd and Cu-Pt Alloys," Corrosion Science 8, 1959.
13. C. Wagner, "Reaktionstypen bei der Oxydation von Legierungen," Z. Elektrochemie, 63, 1959, p. 772.
14. R.A. Rapp, "Kinetics Microstructures and Mechanism of Internal Oxidation—Its Effect and Prevention in High Temperature Alloy Oxidation," Corrosion 21, 1965, p. 382.
15. R.A. Rapp, "Internal Oxidation of Alloys," Encyclopedia of Materials Science and Engineering 3, M.B. Bever, ed. Pergamon Press, Oxford, England, 1986, p. 2374.
16. J.H. Swisher, "Internal Oxidation," Oxidation of Metals and Alloys, D.L. Douglass, ed., ASM International, Materials Park, Ohio, 1971, p. 235.
17. T. Yonezawa and K. Onimura, "Effect of Chemical Compositions and Microstructure on the Stress Corrosion Cracking Resistance of Nickel Base Alloys in High Temperature Water," International Conference on Evaluation of Materials Performance in Severe Environments: EVALMAT '89, The Iron and Steel Institute of Japan, 1989, p. 235.
18. R.H. Bricknell and D.A. Woodford, "The Mechanism of Cavity Formation During High Temperature Oxidation of Nickel," Acta Metallurgica 30, 1982, p. 257.
19. R.G. Iacocca and D.A. Woodford, "The Kinetics of Intergranular Oxygen Penetration in Nickel and Its Relevance to Weldment Cracking," Metallurgical Transactions A 19A, 1988, p. 2305.
20. R. Barlow and P.J. Grundy, "The Determination of the Diffusion Constants of Oxygen in Nickel and γ -Iron by an Internal Oxidation Method," Journal of Materials Science 4, 1969, p. 797.
21. H. Ghonem and D. Zheng, "Depth of Intergranular Oxygen Diffusion During Environment - Dependent Fatigue Crack Growth in Alloy 718," Materials Science and Eng. A150, 1992, p. 151.
22. A. Diboine and A. Pineau, "Creep Crack Initiation and Growth in Inconel 718 Alloy at 650° C.," Fatigue and Fracture of Eng. Mater. Struc. 109, 1987, p. 141.

23. J.A. Pfaendtner, R.C. Muthiah, C.T. Liu, and C.J. McMahon Jr., "Time-Dependent Interfacial Failure in Metallic Alloys," Materials Science and Engineering A260, 1999, p. 1.
24. M.M. Morra, S. Nicol, L. Toma, I.S. Hwang, M.M. Steeves, and R.G. Ballinger, "Stress Accelerated Grain Boundary Oxidation of Incoloy Alloy 908 in High Temperature Oxygenous Atmospheres," Advances in Cryogenic Eng. 40, 1994, p. 1291.
25. F.L. Carranza and R.B. Haber, "A Numerical Study of Intergranular Fracture and Oxygen Embrittlement in an Elastic - Viscoplastic Solid," Mechanics and Physics of Solids 47, 1999, p. 27.
26. D.L. Douglass, "The Effect of Oxidation on the Mechanical Behavior of Nickel at 600°C," Materials Science and Engineering 3, 1968, p. 255.
27. Y. Shida, G.C. Wood, F.H. Stott, D.P. Whittle, and B.D. Bastow, "Intergranular Oxidation and Internal Void Formation in Ni-40% Cr Alloys," Corrosion Science 21, 1981, p. 581.
28. D.P. Whittle, Y. Shida, G.C. Wood, F. H. Stott, and B.D. Bastow, "Enhanced Diffusion of Oxygen During Internal Oxidation of Nickel-Base Alloys," Philosophical Magazine A 46, 1982, p. 931.
29. G.C. Wood, F.H. Stott, D.P. Whittle, Y. Shida, and B.D. Bastow, "The High Temperature Internal Oxidation and Intergranular Oxidation of Nickel Chromium Alloys," Corrosion Science 23, 1983, p. 9.
30. F.H. Stott, G.C. Wood, D.P. Whittle, B.D. Bastow, Y. Shid, and A. Martinez-Villafane, "The Transport of Oxygen to the Advancing Internal Oxide Front During Internal Oxidation of Nickel Base Alloys at High Temperature," Solid State Ionics 12, 1984, p. 365.
31. T.S. Gendron, Intergranular Oxidation as a Mechanism of Stress Corrosion Cracking of Nickel-Base Alloys in High Temperature De-oxygenated Water, University of Manchester Institute of Science and Technology Thesis, Degree of Doctor of Philosophy, Manchester, United Kingdom, 1999.
32. T.S. Gendron, S.J. Bushby, and I.J. Muir, "SIMS Evaluation of Steam Generator Tubing for Evidence of Internal Oxidation," The Ninth International Conference on Environmental Degradation of Materials in Nuclear Power Systems – Water Reactors, Eds. S. Bruemmer and P. Ford, The Mineral, Metals, and Materials Society (TMS), Warrendale, Pennsylvania, 1999, p. 79.
33. T.S. Gendron, P.M. Scott, S.M. Bruemmer, and L.E. Thomas, "Internal Oxidation as a Mechanism for Steam Generator Tube Degradation," Third International Steam Generator and Heat Exchanger Conference, R.L. Tapping, chair., Canadian Nuclear Society, Toronto, Ontario, Canada, 1998, p. 389.

34. T.S. Gendron, S.J. Bushby, R.D. Cleland, and R.C. Newman, "Oxidation Embrittlement of Alloy 600 in Hydrogenated Steam at 400°C," Analysis 25, June 1997, p. M24.
35. T.S. Gendron, R.D. Cleland, and R.C. Newman, "Oxidation Embrittlement of Grain Boundaries in Nickel Alloys," Corrosion '95, Paper 181, 1995, p. 181/1.
36. T. Cassagne, A.-F. Gourgues, and A. Gelpi, "Corrosion Sous Contrainte de L'alliage 600: Les Mécanismes en Question," Revue de Metallurgie-CIT / Sciences et Genie des Materiaux, 90, 1993, p. 1165.
37. Proceedings of the 1987 Workshop on the Mechanism of Primary H₂O IGSCC; NP-5987-SP, G. Economy, R.J. Jacko, J.A. Begley, and F.W. Pement, eds., EPRI, Palo Alto, California, 1987.
38. T. Shoji, "Mechanics and Mechanisms of Stress Corrosion Cracking of Alloy 600 in High Temperature Waters," Proceedings: Specialist Meeting on Environmental Degradation of Alloy 600, EPRI TR-104898, Eds. R.G. Ballinger, A.R. McIlree, and J.P.N. Paine, EPRI, Palo Alto, California, 1996, p. 18/1.
39. R.W. Staehle and J.A. Gorman, "Progress in Understanding and Mitigating Corrosion of the Secondary Side in PWR Steam Generators," Addendum to the Proceedings of the Tenth International Symposium on Environmental Degradation of Materials in Nuclear Power Systems - Water Reactors, P. Ford, G. Was, and L. Nelson, eds., NACE, Houston, Texas, 2002.
40. C.M. Chen, K. Aral, and G.J. Theus, Computer Calculated Potential-pH Diagrams to 300°C: Volumes 1-3; NP-3137, EPRI, Palo Alto, California, 1983.
41. N. Totsuka and Z. Szklarska-Smialowska, "Hydrogen Induced IGSCC of Ni-Containing FCC Alloys in High Temperature Water," Proceedings of the Third International Symposium on Environmental Degradation of Materials in Nuclear Power Systems—Water Reactors, G.J. Theus and J.R. Weeks, eds., The Mineral, Metals, and Materials Society (TMS), Warrendale, Pennsylvania, 1988, p. 691.
42. P.M. Scott and P. Combrade, "On the Mechanisms of Secondary Side PWR Steam Generator Tube Cracking," Eighth International Symposium on Environmental Degradation of Materials in Nuclear Power Systems -Water Reactors, A.R. McIlree, chair., American Nuclear Society, Chicago, Illinois, 1997, p. 65.
43. D.S. Morton, S.A. Attanasio, and G.A. Young, "Primary Water SCC Understanding and Characterization Through Fundamental Testing in the Vicinity of the Nickel/Nickel Oxide Phase Transition," Proceedings of the Tenth International Symposium on Environmental Degradation of Materials in Nuclear Power Systems - Water Reactors, P. Ford, G. Was, and L. Nelson, eds., NACE, Houston, Texas, 2002.

44. D.H. Lee, M.S. Choi, and U.C. Kim, "The Effect of Hydrogen on the Stress Corrosion Cracking of Alloy 600 in Simulated PWR Primary Water at 330°C." Proceedings of the Tenth International Symposium on Environmental Degradation of Materials in Nuclear Power Systems - Water Reactors, P. Ford, G. Was, and L. Nelson, eds., NACE, Houston, Texas, 2002.
45. N. Totsuka, M. Kamaya, N. Nakajim, H. Mitsuda, and S. Sakai, "A New Evaluation Method for Short Crack Growth and Influence of Dissolved Hydrogen on PWSCC of Alloy 600," Proceedings of the Tenth International Symposium on Environmental Degradation of Materials in Nuclear Power Systems - Water Reactors, P. Ford, G. Was, and L. Nelson, eds., NACE, Houston, Texas, 2002.
46. P.L. Andresen and T.M. Angeliu, "Evaluation of the Role of Hydrogen in SCC in Hot Water; Paper #195," Corrosion '97, NACE, Houston, Texas, 1997, p. 195/1.
47. P.L. Andresen, "Conceptual Similarities and Common Predictive Approaches for SCC in High Temperature Water Systems," Corrosion '96, Paper 258, 1996, p. 258/1.
48. J.W. Park and C.J. Altstetter, "The Diffusion and Solubility of Oxygen in Solid Nickel," Metallurgical Transactions A 18a, 1987, p. 43.
49. F.P. Ford and P.L. Andresen, "Corrosion in Nuclear Systems: Environmentally Assisted Cracking in Light Water Reactors," Corrosion Mechanisms in Theory and Practice, P. Marcus and J. Oudar, eds., Marcel Dekker, New York, 1995, p. 501.
50. G. A. Bickel, D. Guzonas, W. Hocking, K. Irving, A. Lockley, I. Muir, F. Szostak, and M. Wright, Examination of Steam Generator Tube Samples from the Upper Bundle Free Span Regions of Oconee Units 1, 2 and 3 Once Through Steam Generators: RC-2348, Chalk River Laboratories, Ottawa, Ontario, Canada, May, 2000.
51. N. Lewis, S.A. Attanasio, D.S. Morton, and G.A. Young, "Stress Corrosion Crack Growth Rate Testing and Analytical Electron Microscopy of Alloy 600 as a Function of Pourbaix Space and Microstructure," Proceedings: Chemistry and Electrochemistry of Stress Corrosion Cracking: A Symposium Honoring the Contributions of R.W. Staehle, R.H. Jones, ed., The Mineral, Metals, and Materials Society (TMS), Warrendale, Pennsylvania, 2001, p. 421.
52. R.B. Rebak, Z. Xia, and Z. Szklarska-Smialowska, "Effect of Temperature and Cold Work on the Crack Growth Rate of Alloy 600 in Primary Water," Corrosion, Vol. 51, 1995, p. 689.
53. H.W. Pickering and Y.S. Kim, "De-alloying at Elevated Temperatures and at 298K—Similarities and Differences," Corrosion Science, Vol. 22, 1982, p. 621.